available at www.sciencedirect.com

ScienceDirect

www.elsevier.com/locate/brainres

BRAIN RESEARCH

Research Report

Magnetoencephalographic signatures of visual form and motion binding

*Charles Aissani, Benoit Cottereau, Guillaume Dumas, Anne-Lise Paradis, Jean Lorenceau**

CRICM, Cogimage, Université Pierre and Marie Curie, UMR 7225, CNRS, INSERM, 47 Bd de l'Hôpital, 75013 Paris, France

ARTICLE INFO

Article history:
Accepted 20 May 2011
Available online 27 May 2011

Keywords:
SSVEP
Form
Motion
Visual binding
MEG

ABSTRACT

This study investigates neural magneto-encephalographic (MEG) correlates of visual form and motion binding. Steady-state visual evoked fields (SSVEF) were recorded in MEG while observers reported their bound or unbound perception of moving bars arranged in a square shape. By using pairs of oscillating vertical and horizontal bars, "frequency-tagged" at f1 and f2, we identified a region with enhanced sustained power at 2f1+2f2 intermodulation frequency correlated with perceptual reports. Intermodulation power is more important during perceptual form/motion integration than during the perceptual segmentation of the stimulus into individual component motions, indicating that intermodulation frequency power is a neuromarker of form/motion integration. Source reconstruction of cortical activities at the relevant frequencies further reveals well segregated activity in the occipital lobe at the fundamental of the stimulation, f1 and f2, widely spread activity at 2f1 and 2f2 and a focal activity in the medial part of the right precentral sulcus region at the intermodulation component, 2f1+2f2. The present findings indicate that motion tagging provides a powerful way of investigating the processes underlying visual form/motion binding non-invasively in humans.

1. Introduction

Vision is a process distributed in numerous, densely interconnected, cortical areas each dedicated to the analysis of particular features (Van Essen et al., 1992; Wandell et al., 2007). Accordingly, a single visual stimulus characterized by several dimensions (e.g. motion, orientation, color) elicits activity in specific, distant areas. Within a single area, distinct neuronal populations sharing the same feature selectivity can be similarly recruited by a single visual object or by several independent objects. Perceiving independent perceptual units thus calls for mechanisms able to selectively link neuronal activity into distinct "neuronal assemblies" within and across areas, an issue widely known as the "Binding Problem" (Milner, 1974; Singer and Gray, 1995; Treisman and Gelade, 1980). Binding-by-Convergence (BBC) and Binding-by-Synchrony (BBS) have been proposed as potential solutions to the binding problem (Barlow, 1972; Fries et al., 2001; Singer and Gray, 1995). Although these two views have been extensively discussed (see Neuron special issue, 1999), it is possible that both contribute to solving the binding problem (Fries, 2009; Varela et al., 2001). In this perspective, neural synchronization in the gamma-band (GB), often considered as a signature of perceptual binding (Gray et al., 1989; Tallon-Baudry and Bertrand, 1999), would optimize the information transfer across hierarchically distributed cortical areas (Fries, 2009; Tallon-Baudry, 2009). However, the functional role of GB activity in visual binding remains an open issue because some studies did not find GB activity or found

* *Corresponding author*. Fax: +33 1 45 86 25 37.
E-mail address: jean.loreanceau@upmc.fr (J. Lorenceau).

0006-8993/$ – see front matter © 2011 Published by Elsevier B.V.
doi:10.1016/j.brainres.2011.05.051

decreased rather than increased GB power (Lima et al., 2010; Palanca and DeAngelis, 2005). The reasons for this discrepancy is unclear but however suggests that observing GB activity may depend upon stimulus features (Friedman-Hill et al., 2000; Henrie and Shapley, 2005), task and attention (Fries et al., 2002), or recorded signals (EEG versus MEG; Tallon-Baudry et al., 1997). More recently, studies brought evidence for a correlation between miniature eye-movements and gamma-band activity (Bosman et al., 2009; Dimigen et al., 2009; Yuval-Greenberg et al., 2008). Thus, GB activity may not always be a reliable marker of perceptual binding (Herrmann et al., 2004b; Jensen et al., 2007).

In this study, we uncover neural magnetoencephalographic correlates of perceptual binding by taking advantage of the 'aperture diamond paradigm' (Lorenceau and Shiffrar, 1992) in which periodic oscillations of disconnected bars arranged in a square shape can be perceived as either a single moving shape or as unbound moving segments. With these displays, the local oscillatory motion of the bars recruits direction selective neurons in different locations whose responses are phase-locked to the fundamental or harmonics of the stimulation frequency for long periods of time (Ales and Norcia, 2009; Pei et al., 2002). Such synchronized responses reflect on the human scalp as reliable oscillatory signals endowed with a high signal-to-noise ratio (Steady-State Visual Evoked Potential, SSVEP, for EEG or Field SSVEF for MEG), characterized by narrow and well-defined peaks in their Fourier transform, which correspond to the stimulation frequency or some of its harmonics, depending on the displays (e.g. flicker or counter-phase temporal modulation). Using stimuli composed of different frequencies (e.g. f1 and f2) yields complex evoked spectra not only comprising frequencies related to the periodic stimulations but also intermodulation terms (nf1 ± mf2) which have been proposed to reflect interactions between specific neural groups (Appelbaum et al., 2008; Regan and Regan, 1988; Victor and Conte, 2000; Zemon and Ratliff, 1984). For example, when two orthogonal gratings flickering at different temporal frequencies – f1 and f2 – are presented in binocular rivalry (one in each eye), EEG recordings reveal enhanced power at the f1 + f2 intermodulation frequency when the two images are perceived as combined (Sutoyo and Srinivasan, 2009). This and other results (Appelbaum et al., 2008) support the notion that perceptual integration can be reflected in the intermodulation frequency terms.

With our displays, seeing a bound moving square requires the perceptual integration of oscillatory bar motions corresponding, at the physiological level, to integrating responses to component motion in primary visual cortex – where orientation and direction selective neurons have small receptive fields – by higher-order neurons. Using different oscillation frequencies for each pair of bars and assuming that activity in higher-order neurons reflects the temporal structure of their inputs, we predict a power enhancement at the intermodulation frequencies when bar motions are perceptually integrated into a bound moving figure. More precisely, we hypothesize that an oscillatory motion at a frequency f1 (respectively f2) will elicit neural activity at 2f1 (respectively 2f2) in primary visual cortex, because the architecture of models of motion processing includes a rectification or squaring term (Rust et al., 2006; Simoncelli and Heeger, 1998) whose effect is to double the input frequency. Further, combining the responses from primary visual cortex in higher order regions involves a non-linear operation expected to appear at intermodulation terms, mostly 2f1 + 2f2. According to this scheme, changes in the power at 2f1 + 2f2 may bring a neural signature of whether component motions were or not bound into a unified motion percept.

To induce different bound/unbound percepts, we relied on previous psychophysical studies showing that high contrast bar-ends favor motion segmentation while low contrast bar-ends favor motion integration (Lorenceau and Shiffrar, 1992; Lorenceau et al., 1993; Lorenceau and Zago, 1999). Electrophysiological studies further showed that surround suppression in end-stopped V1 neurons was strongly modulated by contrast (Sceniak et al., 1999; Yazdanbakhsh and Livingstone, 2006) and that end-stopping played a gating role in motion integration (Guo et al., 2006; Pack et al., 2003; Sceniak et al., 1999). It is therefore likely that perceptual integration into bound or unbound percepts is rooted in the modulation of end-stopped V1 responses.

In the following, the MEG recordings performed while participants classified their perception of these motion displays are analyzed in details to identify and test several candidate markers of visual form/motion binding. Although the experimental design was primarily conceived to investigate the relationships between perceptual reports and the SSVEF response at fundamentals, harmonics, and intermodulation components of the motion stimulus, we also analyzed and contrasted induced activity elicited by the two percepts in the gamma band.

2. Results

2.1. *Behavioral results*

The averaged distribution of observers' responses is presented in Fig. 2 as a function of the 4 luminance conditions. Clearly, observers mostly perceived a rigid moving square when line-end luminance was low and perceived disconnected moving segments when line-end luminance was high. Overall, only few trials remained unclassified, suggesting that observers reliably identified one or the other perceptual state over the duration of a trial. Note that whereas line-end luminance increases linearly across the first three conditions (Fig. 1), observers' judgments show a discontinuity in the bound/unbound classification between conditions 2 and 3, showing that a small change in bar-end luminance entails large perceptual modifications. An ANOVA (3 × 4 factors) conducted on these data indicated a significant interaction between perception and condition ($p < 10^{-15}$). Additional analyses for each percept (1 factor, 4 conditions) showed a significant effect of the conditions on the response rate for the bound and unbound percepts ($p < 10^{-13}$ and $p < 10^{-14}$ respectively) but not for unclassified percepts ($p > 0.43$).

2.2. *MEG results*

MEG results will be presented in two sections: the first one concerns evoked fields recorded around relevant frequencies. Cluster-based analyses (see Experimental procedures) were performed on the last 1030 ms of moving stimulation to avoid contamination of the spectral analyses by the transient motion onset response.

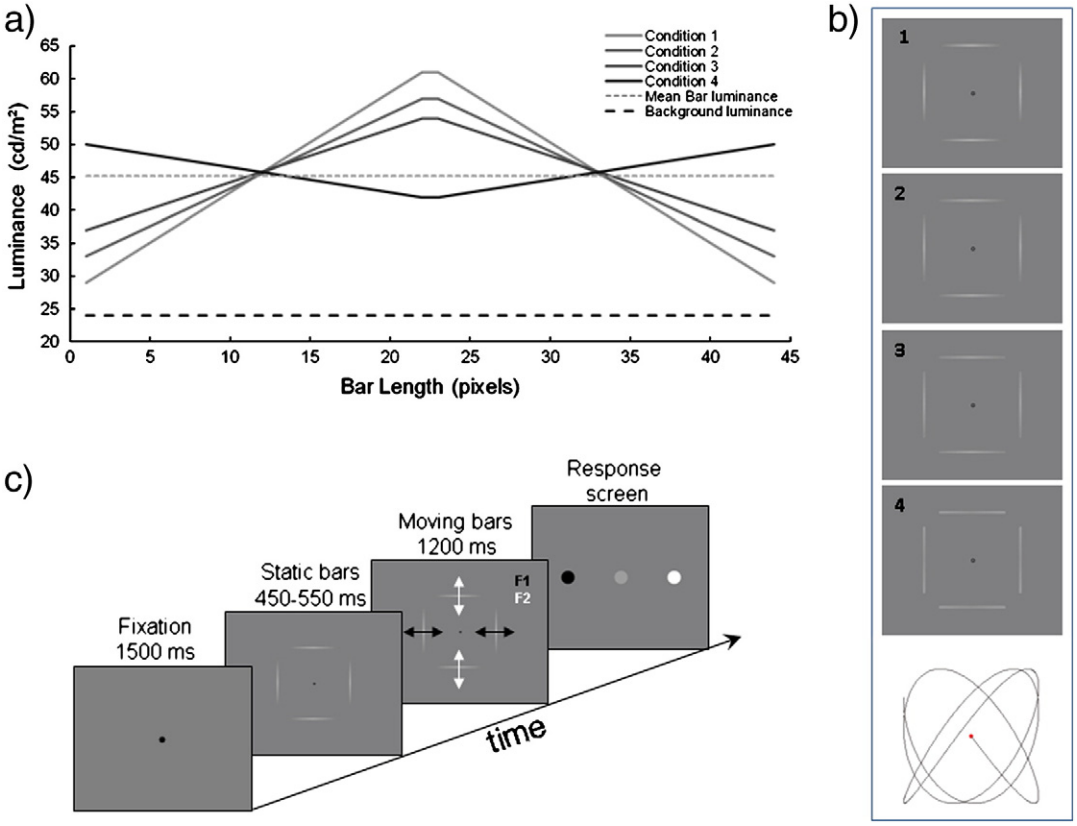

Fig. 1 – Stimuli and protocol. a) Distributions of luminance along the bars used to elicit different percepts for each condition: from strongly bound (condition 1, darkest gray) to completely unbound (condition 4, lightest gray). All four bars had the same luminance profile; the mean bar luminance of the bars (dotted line) was the same across conditions. b) Snapshots of the four conditions used in the study and of the full motion trajectory during the 1.2 s of stimulation. c) Time flow of a trial. A homogenous background (baseline) was followed by the presentation of a static stimulus (between 450 and 550 ms) and by the motion stimulation (1200 ms). The response screen appearing at the end of the stimulation indicated the possible choices: black for bound, white for unbound and gray for unclassified. The disks changed position on each trial to avoid motor preparation during stimulus motion.

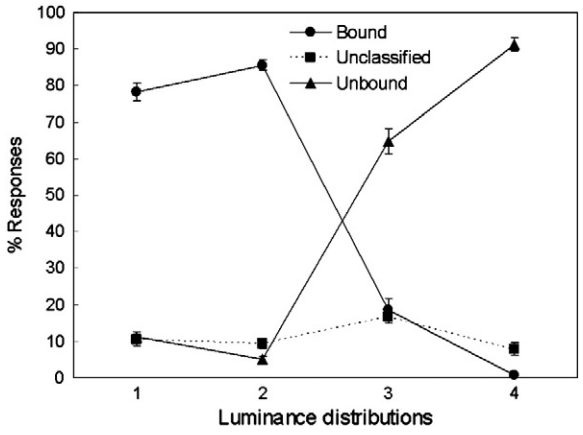

Fig. 2 – Averaged (n=10) response rates as a function of the different luminance distributions for bound, unbound and unclassified percepts. Error bars represent ±1 standard error of the mean.

We first present results computed on all trials, independently of observers' perception to assess the efficacy of frequency tagging. We then contrast bound and unbound evoked activity at the stimulation frequencies, their first harmonics and the intermodulation product 2f1+2f2 and present the sources reconstructed using a minimum norm approach.

A second section investigates gamma induced activity computed independently of observers' percepts to isolate the most relevant frequency band which is then used to contrast trials seen as bound or unbound so as to determine whether gamma activity provides a signature of perceptual binding.

2.2.1. Activity at the fundamental and harmonics of the motion tagging frequencies

To determine which cortical regions are stimulated by bar motion and ensure that our stimuli elicit sustained frequency-tagged responses, we computed the evoked fields independently of the experimental conditions or observers' reports. The high signal-to-noise ratio of SSVEF associated with the oscillating

bars provides a reliable estimate of the activity common to all conditions.

The power topography at the fundamental and first harmonics recorded on the MEG sensors (Fig. 3a) indicates that activity at the two fundamental frequencies of bar motion is more posterior and more focal than activity at the two 1st harmonics, 2f1 and 2f2. The greater activity found for these 1st harmonics is widely spread across different cortical regions. In addition, the time–frequency plots (Fig. 3b, example from an occipital sensor) shows that the oscillatory motion indeed elicits sustained activity at the expected frequencies.

We more precisely localized the spatial distribution of fundamental and 1st harmonic activities by reconstructing the sources of the MEG signals on Collin MNI, while taking into account the head position measured for each subject and each run (see Experimental procedures for details). The reconstructed sources, presented in Fig. 4, reveal a widely-distributed significant activity, mainly along the dorsal pathway, with some activity in the ventral stream for the 1st harmonic.

Only a small percentage of sources showed significant activity at more than one frequency: 7.9% activated at both f1 and f2, and 6.9% at 2f1 and 2f2; for these however, only the frequency yielding the most significant power was represented.

Notably, the activity related to f1 and f2 reveals a clear retinotopic segregation in the occipital lobe (Fig. 4c), congruent with the localization of the stimulus in the visual field: sources associated to the vertical bars moving along the horizontal meridian (tagging frequency f1, yellow sources), are predominantly found along the calcarine sulcus, while sources related to horizontal bars moving along the vertical meridian (tagging frequency f2, red sources) are predominantly distributed above and below the calcarine sulcus, as expected from the known retinotopic organization of early cortical areas in humans (Wandell et al., 2007).

A quantitative estimation of the number of sources reveals a predominance of f2 and 2f2 activity (Fig. 4b) as compared to the f1 and 2f1 activity. The weak overlap between the sources activated by different tagging frequencies, (see Fig. 4b f1 & f2 and 2f1 & 2f2) indicates that the two pairs of bars activated well-segregated areas within the occipital lobe.

We next seek whether the different perceptual states modulate activities at the fundamental and harmonics of the oscillatory motions, by contrasting the power elicited by the stimuli at the fundamentals (f1 and f2) or at the first harmonics (2f1 and 2f2) for the bound and unbound percepts. These analyses were conducted on all sensors and did not

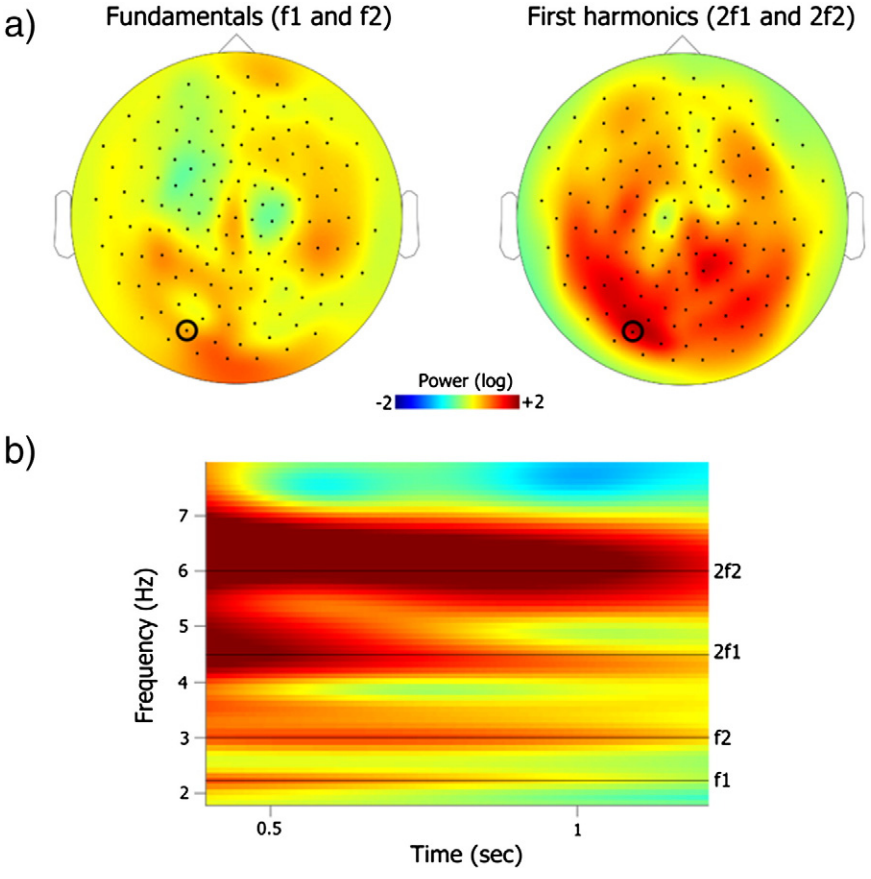

Fig. 3 – *Top*: Topographies of the steady-state response during the motion stimulation averaged across trials and observers. The color map represents the mean power – relative to baseline – at the two fundamentals (f1 and f2, left) and first harmonics (2f1 and 2f2, right) of the tagging frequency during the last 1030 ms of stimulation, regardless of the percept reported by the observers. *Bottom*: Time–frequency map of the encircled sensors in a) showing the frequency selectivity of the sustained activities.

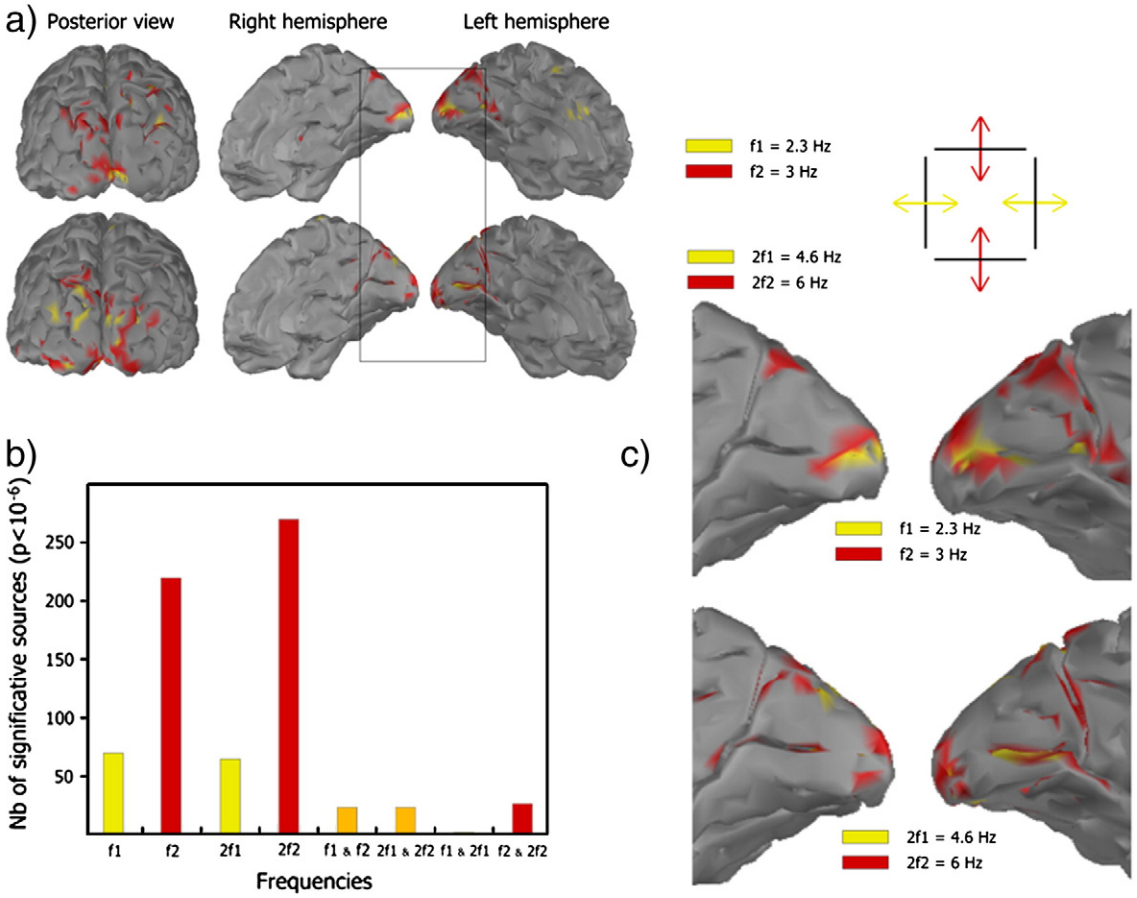

Fig. 4 – a) Significant ($p<0.05$ Bonferonni corrected) sources activated at the fundamental and 1st harmonics of the oscillatory motions displayed on a posterior view and 2 medial views of the right and left hemispheres. The top-right inset indicates the correspondence between the bars and the tagging frequencies. Yellow: f1 and 2f1; red: f2 and 2f2. Sources significantly activated by the two frequencies (f1 and f2 or 2f1 and 2f2), are displayed with the color of the frequency with highest significance. b) Total number of sources above threshold for the different frequencies (f1, f2, 2f1, 2f2), including sources significantly activated by more than one frequency. c) Enlarged medial views of the right and left hemispheres.

reveal any significant power modulation ($p>0.05$). As perceptual classification is correlated to small differences in stimulus luminance, the lack of a significant effect suggests that physical differences did not modulate the responses evoked at early processing stages.

2.2.2. *Activities at 2f1+2f2 intermodulation term*

As described in the introduction the main goal of this study was to test whether the 2f1+2f2 intermodulation term is a specific neuromarker of visual binding. We therefore contrasted the 2f1+2f2 power between trials classified as bound or unbound. This analysis reveals a significant cluster of 3 right frontal sensors (black circles in Fig. 5a) showing power enhancement at 2f1+2f2 (paired t-test, $p<0.05$, corrected).

The time–frequency power averaged across these three sensors (Fig. 5b) is narrow-band around 10.6 Hz and sustained during the motion stimulation suggesting specific computations during both perceptual states. The source reconstruction in Fig. 5c reveals several sources anterior to the precentral sulcus for which 2f1+2f2 activity was enhanced when observers reported a bound percept (paired t-test, $p<10^{-4}$ uncorrected). To further assess the frequency specificity of this result, we performed the same test with a similar threshold for 9.5 and 11.5 Hz but did not find any significant activity in any cortical sources.

2.2.3. *Gamma band activity*

Previous studies (Singer and Gray, 1995; Tallon-Baudry and Bertrand, 1999; Varela et al., 2001) suggest that synchronization in the gamma band (GB) is a neural signature of visual binding. According to this hypothesis, in our study, induced GB power in bound trials should be enhanced as compared to unbound trials. We therefore computed the trial-by-trial frequency power for each percept and each observer. We first determined the frequency band of interest by performing a time–frequency analysis over motion stimulation for all trials. As the GB power was greatest between 55 and 85 Hz (Fig. 6b), we averaged GB activity in this frequency range

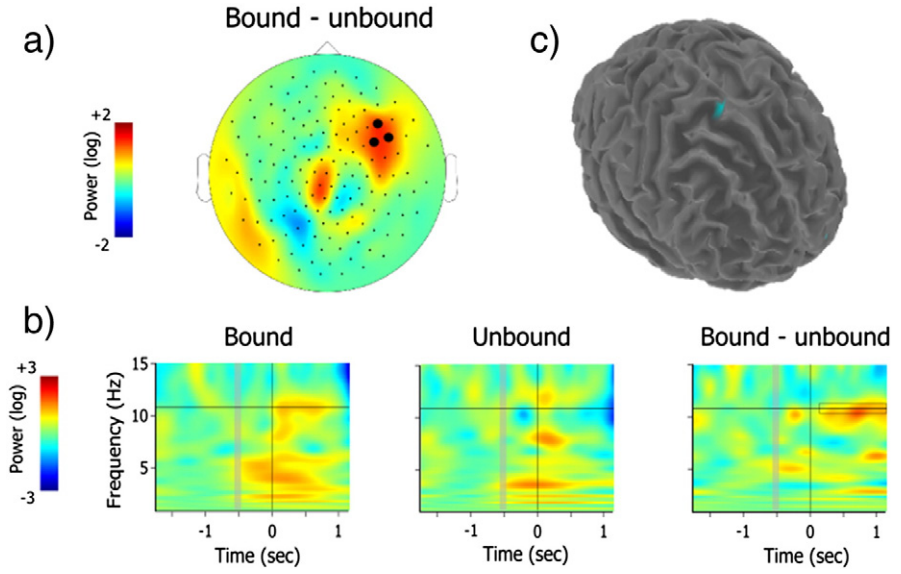

Fig. 5 – Intermodulation frequency (2f1 + 2f2, 10.6 Hz) and percept-dependent activity. a) Topography of the power-log difference around 10.6 Hz between bound and unbound states. The black disks indicate sensors with significant differences ($p < 0.05$, paired t-test, corrected). b) Averaged time–frequency plot of the evoked signal (SSVEP) for the bound and unbound percepts and for their difference across the three frontal sensors shown in a). Time zero corresponds to motion onset; the gray bar around −0.5 s indicates the time range at which the static bars appeared across the trials (variable durations of the static display, see Experimental procedures); horizontal lines signal the 10.6 Hz frequency. The black rectangle indicates the time–frequency window of interest. c) Source reconstruction of the significant 10.6 Hz enhancement during bound percepts relative to unbound percepts ($p < 10^{-4}$, paired t-test).

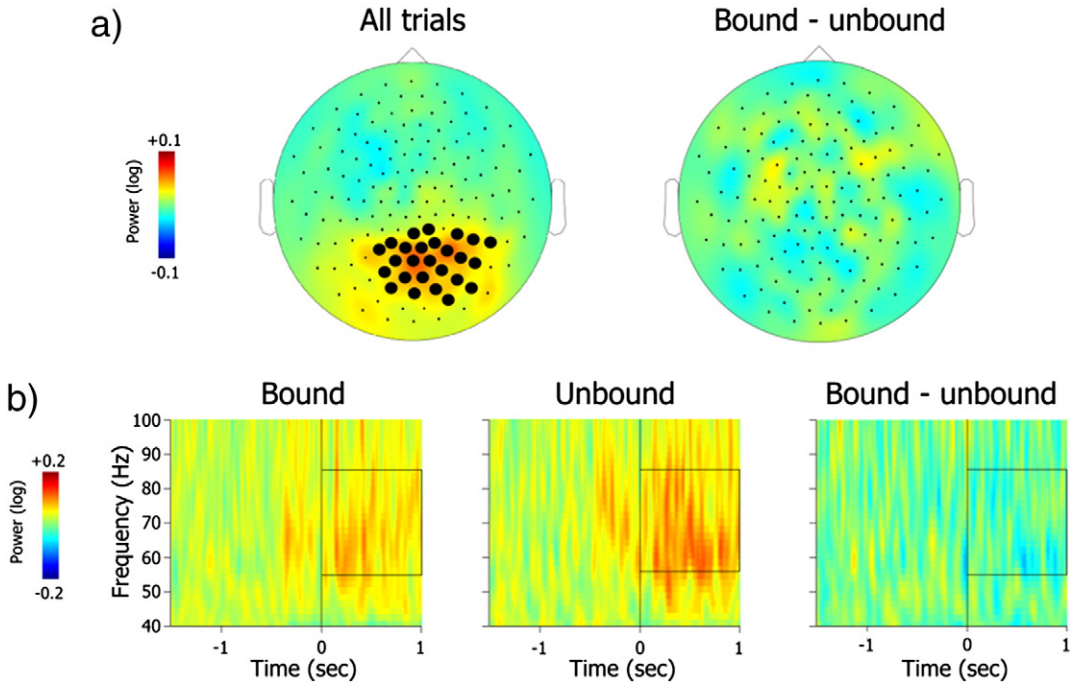

Fig. 6 – Induced gamma activity. a) Gamma power averaged between 55 and 85 Hz. Left: topography computed from all trials. Black disks indicate the sensors with significant gamma modulation ($p < 0.05$, corrected). Right: topography of the difference in gamma power between bound and unbound percepts. b) Time–frequency plots of gamma activity for bound (left), unbound (center) trials and their differences (right) averaged across the sensors shown in a). The black rectangle indicates the time–frequency windows used for the analysis.

across trials. A cluster of numerous occipital and parietal sensors shows significant GB activity during the motion stimulation ($p<0.05$ corrected; left topography in Fig. 6a). However, the difference in GB activity between bound and unbound trials was not significant ($p>0.05$; right topography in Fig. 6a). Thus, in this study, GB modulation did not appear as a reliable neural marker of perceptual binding. Note that taking the correlation between eye-movements and GB activity (Yuval-Greenberg et al., 2008) at face value suggests eye-movements that may have differentiated trials seen as bound or unbound were similar. This, however, does not preclude the possibility that the MEG activity and residual eye-movements that may have survive the removal of trials with eye-signals are somehow correlated, a possibility investigated in detail in the following section.

2.3. *Oculomotor control*

Are eye-movements correlated to oscillatory stimulus motion and MEG activity? To address this issue, we considered both the saccade rate and the time–frequency power of eye traces that may reveal undetected miniature eye-movements possibly correlated to the frequency modulation found in the MEG data. We first compared the number of saccades on the raw traces (before saccades removal) for the two perceptual states. This analysis did not reveal any significant difference between trials seen as bound or unbound ($p>0.15$, paired t-test). We then performed the same analyses as for the MEG signals on eye traces. Because eye-traces were of poor quality in two observers due to head shifts and since vertical eye-traces have lower resolution than the horizontal ones with our eye-tracker device, this analysis was conducted on eight observers and horizontal eye-traces only. However, to increase the number of trials included in this analysis and to improve the statistical power, we included trials that were previously rejected because they were contaminated by eye-movements during the base-line. We then averaged all trials for each percept and observers and computed the power spectrum of eye traces around all frequencies of interest. Comparing the time–frequency power for trials seen as bound and unbound did not reveal any significant difference ($p>0.21$, paired t-test) suggesting that, on averaged, intrusive eye-movements were unlikely to account for the differences found in the MEG signals. However, inspecting the individual results revealed inter-individual differences: some observers showed sustained power enhancement at the fundamental of the stimulus oscillation while others showed a decreased power in the bound/unbound comparison. No such power enhancement was found at any other frequency, in particular at the intermodulation frequency term that differentiates the bound/unbound MEG data. We however decided to seek whether individual eye-data would correlate to intermodulation power.

Fig. 7 presents the power modulation averaged over motion duration for eye-traces and the 10.6 Hz intermodulation frequency (averaged across the frontal sensors found) for each observer. As it can be seen, the correlation between both measures is weak ($R^2=-0.062$), indicating that observers showing a large difference at the intermodulation frequency were not necessarily those with larger eye-traces modulations. Overall, these analyses suggest that eye-movements do not account for the differences found in the MEG data.

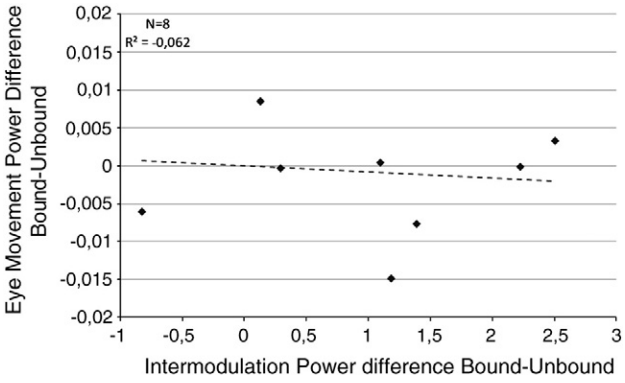

Fig. 7 – Correlation between differential horizontal eye movement power at 2.3 Hz and differential intermodulation power averaged on the three significant frontal sensors shown in Fig. 5.

3. Discussion

Using visual displays endowed with oscillatory motions and yielding different perceptual states – a bound moving square versus independently moving bars – we identified neural activities reflecting visual processing independent of the perceptual states — namely activities at the fundamental and harmonics of the oscillatory motions and activities correlated to the observers' perceptual reports, characterized by a different power at the 10.6 Hz intermodulation frequency ($2f1+2f2$). In the following, we discuss the possible origins of these activities and the implications of these results.

3.1. *Stimulus versus perception-driven responses*

The different stimuli used in this study differed only by small differences in the distribution of luminance along the bars, mean luminance being identical in all conditions. As perceptual reports and the different luminance distributions are tightly correlated, the MEG results may reflect both stimulus-driven responses and their perceptual counterparts. It is however unlikely that observers relied on these physical differences to perform the task. As a matter of fact, when asked at the end of the experiment what distinguished the experimental conditions, only one observer (not included in the analyses) among twelve reported luminance as a factor. This is expected if observers attended, as prompted, to their bound/unbound perception rather than to luminance differences. Moreover, the bound/unbound phenomenal differences are highly salient and spontaneously reported by observers when discovering the stimuli. Moreover, numerous studies demonstrated (e.g. Carrasco et al., 2004; Reynolds et al., 2000) that attending to a specific feature enhances the strength of the responses to this feature (and consequently at the tagged-frequencies, Pei et al. 2002). In accordance with these studies, our MEG results are likely to reflect activity in the circuits involved by a task bearing on global salient characteristics rather than on an

otherwise local unnoticed feature, despite the fact that this very feature drives perception. In this regard, our behavioral results replicate and extend previous psychophysical studies (Lorenceau and Shiffrar, 1992) showing that high contrast line-ends favor motion segmentation while low contrast line-ends favor motion integration. This perceptual outcome is compatible with the finding that surround suppression in end-stopped V1 neurons is modulated by contrast (Sceniak et al., 1999; Yazdanbakhsh and Livingstone, 2006) and that end-stopping plays a gating role in motion integration (Pack et al., 2003; Sceniak et al., 1999; Yazdanbakhsh and Livingstone, 2006). It is therefore likely that observers' classification into bound or unbound trials is rooted in modulation of end-stopped V1 responses. The large behavioral differences observed between the physically very similar conditions 2 and 3 further indicate the high sensitivity of perceptual binding to these subtle contrast changes. As the analyses were performed on behavioral results rather than on physical differences, we shall refer to perceptual binding when discussing the results.

3.2. *Activities at the fundamentals and harmonics of the motion frequency stimulation*

In our displays, the vertical and horizontal line segments oscillated at two different frequencies. Source reconstruction at these frequencies revealed a clear segregation in primary visual cortex: horizontally moving bars elicited activity along the calcarine fissure while the sources corresponding to the vertically moving bars fell on both sides of the calcarine fissure, a finding consistent with their respective position in space motion axis and the known retinotopic organization of V1 (Wandell et al., 2007). Frequency-tagged moving stimuli thus offer a "spectral scout" to isolate relevant cortical signals in an otherwise over rich spectrum of neural activities (Swettenham et al., 2009). This result legitimates the use of SSVEF/MRI in source reconstruction and indicates how accurate source reconstruction with MEG recordings can be (also see Cottereau et al., 2011).

However, the finding of activity at the fundamental frequency for both the horizontal and vertical bar motions is intriguing. This finding is not easily accounted for by a periodic activity of V1 cells recruited by the oscillatory bar motions. In effect, one expects that non-direction selective neurons tuned to bar orientation fire twice during a full cycle when stimulated by a bar moving back and forth — except at the maxima of the oscillatory motion. On the other hand, although a single V1 direction selective cell should respond once during a cycle, a cell tuned to opposite directions at the same location should respond out-of-phase, eliciting activities at the first harmonic of the stimulation frequency by summation at the MEG sensor level. The strong MEG signal found at the fundamental of the oscillatory motions indicates that this scheme is an over-simplified view. We yet dot not have a convincing explanation of this finding, although the precise localization of the sources of these activities in the occipital pole, their clear segregation in accordance with both their orientation and tagging frequency and their congruency with the expected retinotopic mapping of these sources within primary visual cortex suggest these signals are not artifacts. A recent EEG study (Pei et al., 2002) employing bars moving at tagging frequencies similar to those used herein (2.3 and 3 Hz) also reports activity at the fundamentals of the stimulation, confirming that the present finding is not specific to the particular displays used herein or to the recorded signals (EEG versus MEG). A second intriguing feature of the data is the larger activity found for horizontal bars oscillating at 3 Hz along a vertical path as compared to vertical bars oscillating at 2.3 Hz along a horizontal path. This finding is reminiscent of the imbalance between the processing of horizontal and vertical contours (Aspell et al., 2010; Avery and Day, 1969). A number of studies have found that larger speeds elicited larger MEG response (e.g. Kawakami et al., 2002; Lam et al., 2000). It is however unlikely that the larger maximal speed of the vertical motion can account for this imbalance as the difference in speed remains small during motion. One tentative explanation of this difference is that horizontal bars crossing the vertical meridian recruit homotopic neurons from both hemispheres whose joint activity may have enhanced the MEG signal, for instance because of an enhanced synchronization of homotopic neurons through the corpus callosum (Innocenti, 2009; Nowak et al., 1995).

The cortical sources related to activities at the harmonic frequencies – 2f1 and 2f2 – reveal a wide distribution that spans several cortical areas, mostly in the dorsal pathway. The more occipital activities at the fundamental frequencies and the spread of activities at the first harmonics suggests that visual neurons, presumably within V1, transform the incoming signals in a way that entail a doubling of the input frequencies in extra-striate areas, a view compatible with computational models of motion processing (Simoncelli and Heeger, 1998) that include a non-linear squaring rectification term.

Source localization was performed using the trials from all experimental conditions. Despite the good signal-to-noise ratio of the SSVEF and the precise localization of its sources, contrasting further activities at the fundamental and at the first harmonics of the stimulation for bound and unbound percepts yields non-significant differences. Although various reasons may account for the lack of significance, it is worth noting that the different stimulus conditions were only physically marginally different (Fig. 1). The sharp perceptual differences they nevertheless induced (See Supplementary movies), for instance between conditions 2 and 3, suggest non-linear transformations underlie these well segregated percepts. As mentioned above, converging lines of evidence indicate that line-ends' processing is at the core of this phenomenon (Lorenceau and Shiffrar, 1992) as end-stopping is also modulated by contrast changes (Pack et al., 2003; Sceniak et al., 1999; Yazdanbakhsh and Livingstone, 2006) and control motion integration (Tsui et al., 2010). The present results however failed at finding significant neural correlates of this process at the tagging-related frequencies used herein.

3.3. *Intermodulation frequency or alpha rhythm?*

The finding of an enhanced focal activity at the 2f1+2f2 intermodulation term in bound relative to unbound trials is compatible with models of motion integration according to which a non-linear combination of the two harmonic frequencies underlies perceptual binding. However, the 10.6 Hz intermodulation term falls within the alpha band (8–13 Hz). Could the activity at this particular frequency reflect observers' alpha rhythm rather than perceptual integration? Several observations

suggest this is unlikely. First, the sustained 10.6 Hz activity is associated to a focal right frontal region, which is at odds with the usual parieto-occipital location of alpha sources. Two studies reported an evoked frontal modulation in the alpha band but found an activity restricted to the left frontal hemisphere during saccade preparation and production (Brignani et al., 2007) or a decrease of evoked alpha on some frontal electrodes during Kanizsa square perception as compared to perceiving isolated "pacman" inducers (Herrmann et al., 2004a). Second, alpha frequency varies with observers' age or cognitive state (Klimesch, 1999; Posthuma et al., 2001). In the present study, the wide distribution of observers' ages (mean age 29.3±9.1) results in a widely spread alpha band activity at the group level (high power during the resting baseline between 8 and 13 Hz on occipital and parietal sensors, data not shown). By comparison, the lack of significant differences between bound and unbound trials at 9.5 Hz and 11.5 Hz suggests that the differential activity centered on the expected intermodulation term at 10.6 Hz is too specific and narrowband to correspond to alpha rhythm. Finally, the 10.6 Hz is locked to motion onset and sustained during stimulus motion. In the studies we aware of, evoked alpha is usually restricted to the first 500 ms of stimulation (Freunberger et al., 2009; Klimesch et al., 2004; Min et al., 2007), is not phase-locked to a steady-state stimulus nor sustained during the whole stimulation. The differential narrow band sustained activity at the 10.6 Hz intermodulation frequency found in a cluster of frontal sensors is therefore more likely to reflect a genuine signature of visual binding.

3.4. *Gamma activity, binding and motion processing*

Since the seminal study by Gray and Singer(1989), the existence and functional role of gamma-band (GB) activity has been thoroughly investigated in humans with EEG or MEG (Fries, 2009; Tallon-Baudry, 2009). Most of these studies found enhanced GB activity when disparate elements are bound into a single meaningful object relative to when they are not. In these studies, the GB modulation was assessed by contrasting objects versus non-objects (Gruber et al., 2006) or familiar versus unfamiliar forms (Busch et al., 2006) that, in addition to visual binding, involved other processes such as object or face recognition (Keil et al., 1999; Rodriguez et al., 1999), texture segregation (Kinsey et al., 2011; Revonsuo et al., 1997) or eye-movements (Yuval-Greenberg et al., 2008). Moreover, the physical differences between the stimuli used to differentiate bound and unbound states are often large and salient. It is therefore uneasy to determine whether perceptual binding per se induces the observed GB modulations or whether GB activity reflects other cognitive processes such as object recognition and associated automatic semantic processes. In our paradigm, the stimuli that entailed bound or unbound percepts differed only by subtle, unnoticed, luminance distributions (Fig. 1). Moreover, the bound or unbound states elicited by these stimuli are equally perceptually relevant and presumably not contaminated by high level cognitive processes: a square moving along a Lissajous' trajectory or two pairs of parallel bars moving independently along orthogonal axes (see Supplementary movies), such that only Gestalt stimulus properties – closure, good continuation, common fate – are perceptually different. This class of stimuli may therefore be better suited to investigate the relationships between perceptual binding and GB activity. However, contrasting activity for trials seen as bound or unbound did not reach statistical significance. This lack of significance differences in GB activity is not due to a lack of GB responses. A peak of GB power recorded along occipito-parietal sensors is expected for a moving stimulation (Friedman-Hill et al., 2000; Henrie and Shapley, 2005) and was indeed found in the present study (Fig. 6a). In previous studies, GB activity with extended gratings or random dot kinematograms was found to depend on motion coherence (Siegel et al., 2007), contrast (Hall et al., 2005), spatial frequency (Hadjipapas et al., 2007) and to shift toward higher frequencies for moving, as compared to static stimuli (Swettenham et al., 2009). As mentioned above, in the present study, stimuli differed by small differences in the luminance distribution that entailed small local changes in contrast, while mean luminance was held constant. In contrast to changes in motion coherence studied with random dot kinematograms that modulate GB activity (Siegel et al., 2007) the temporal frequency and directional content of the stimuli were identical for all conditions and motion detectability was largely above threshold in all cases. Studies on neural synchronization in cat and monkeys mainly used plaid stimuli (Castelo-Branco et al., 2002; Lima et al., 2010; Thiele and Stoner, 2003). Results from these studies are contradictory, some finding enhanced synchronization in the GB for coherent plaids in anesthetized cat (Castelo-Branco et al., 2000) while others failed to replicate these findings in V1 (Lima et al., 2010) or MT (Thiele and Stoner, 2003) in awake monkey. Overall, despite motion stimuli induce strong GB responses, the modulation of these responses by perceptual binding remains an open issue. From the present results with highly similar stimuli eliciting very different percepts, the lack of significant GB modulation by perception suggests it may not be such a reliable marker of perceptual binding, at least with the protocol and stimuli used herein. As attention has been found to modulate the GB response (Fries, 2009), we note that the lack of differences in the GB is at odds with an interpretation of our results in terms of difference in attention allocation between perceptual states.

3.5. *Eye-movements and MEG activity*

Recent studies found that blinks, saccadic or miniature fixation eye-movements were correlated to EEG or MEG responses (Bardouille et al., 2006; Bosman et al., 2009; Yuval-Greenberg et al., 2008). In addition, there is direct evidence from animal studies that neural activity in visual areas may be directly modulated by small fixation eye-movements, including primary visual cortex (Engbert, 2006; Hsieh and Tse, 2009; Kagan et al., 2008; Martinez-Conde et al., 2000; Snodderly et al., 2001). According to these studies, if observers made different eye-movements during the bound and unbound trials, one would expect to find differential activity in these regions depending on perception. Moreover, the previously observed correlation between GB activity and eye-movements (Yuval-Greenberg et al., 2008) would suggest that differences in eye-movement behavior should be reflected in differential GB activity, especially in the 150–350 ms following motion onset. As mentioned above, that GB activity did not differentiate perceptual binding is a first, although indirect, evidence that eye-movements were similar in bound and unbound trials. Dimigen et al. (2009) found EEG correlates of eye movements during a 10 s fixation task, time-locked to miniature

saccades, in the theta and lower alpha frequency bands of occipital sensors and thus very different from the present results. Analyzing eye-movement power during motion stimulation revealed large inter-observer variations restricted to the fundamentals of the stimulus oscillations. However, eye-movement power was not correlated to power at the intermodulation term. In a recent study Laubrock et al.(2008) found that the rate of miniature saccades is triggered to the temporal frequency of apparent motion. According to this study, if unnoticed miniature eye-movements had contaminated our data, the rate of miniature saccades should reflect the temporal frequency of the oscillatory motion. As mentioned above the eye-movement time–frequency power was highly variable between observers. When present, it was indeed restricted to the fundamental of the motion oscillation. The finding of enhanced power at 10.6 Hz intermodulation frequency during bound trials in frontal sensors is thus unlikely to be directly related, or caused by, overt eye-movements. It remains possible that covert attentive tracking of stimulus motion has differently modulated neural activity. Indeed, one way to perform the bound/unbound classification is to covertly attempt to pursue the stimulus. Successful covert tracking may entail bound responses while failure to covertly track stimulus motion may entail unbound responses. Although we have no means to determine whether observers used or not this strategy, it would make sense with regard to the task at hand. This interpretation would be in line with the finding of enhanced intermodulation power in frontal sensors as well as with studies of multiple-object-tracking where neural activity in the precentral sulcus is modulated by the number of object to track (Culham et al., 1998; Jovicich et al., 2001). Thus one cannot exclude that our displays elicited different attentional strategies depending on the number of moving objects, a single square shape during bound percepts and four independent bars – or two pairs of bars – during unbound percepts.

3.6. *Intermodulation activity: localization and functional role*

The significant enhancement at the 10.6 Hz intermodulation frequency is restricted to several frontal sensors (Fig. 5a). Source reconstruction of this well defined spectral activity reveals a focal localization on the medial part of the right precentral sulcus (Fig. 5c; Talairach coordinates: x=11.06; y=−23.47; z=73.11).

This finding appears at odd with countless studies and models suggesting that motion integration involves the dorsal pathway and specifically propose that area MT combines the V1 responses to component motion into a coherent pattern motion (Castelo-Branco et al., 2002; Movshon et al., 1985; Simoncelli and Heeger, 1998). However, this view is mostly based on studies using plaid stimuli. A recent electrophysiological study using non-overlapping gratings failed to report motion integration in MT (Majaj et al., 2007). However the high contrast gratings used in this study do not elicit coherent motion percepts in humans (Lorenceau and Zago, 1999), such that it is not easy to determine whether MT neurons integrate non-overlapping component motions. With the non-overlapping moving bars used herein, the contrast between bound and unbound percepts did not elicit significant differences in the dorsal pathway in the frequency range tested. One possibility is that MT receptive fields are too small (less than 4 dva at the eccentricity used here; Gattass and Gross, 1981; Komatsu and Wurtz, 1988; Mikami et al., 1986) to encompass the motion of neighboring bars (3 dva from fixation, bar length 5 dva) so as to drive an intermodulated responses. This is however untrue for the larger MST receptive fields. This does not mean that the MT/MST region was not recruited by our stimuli as activity at the harmonic frequencies lies along the dorsal pathway, but suggests that intermodulation signatures of form/motion integration occur elsewhere.

Given the visual nature of the tagging stimulation and previous functional localizations of frontal regions (Hagler and Sereno, 2006; Paus, 1996), it is possible that the sources of the 10.6 Hz power enhancement identified in the medial part of the right precentral sulcus when contrasting bound and unbound percepts are part of the Frontal Eye Field region (FEF), although they are located slightly more posterior and more medial than that delineated using saccadic eye movements as a functional localizer (Paus, 1996). As the FEF location is linked to similar anatomical landmarks across subjects (Lobel et al., 2001), reconstructing the sources of activity using a single Collin 27 structural MNI, as done here, may introduce localization biases given the large structural inter-subject variability in this region (Lobel et al., 2001; Paus, 1996). Thus the anatomical localization found here should be considered with caution.

However, the existence of reciprocal connections between FEF and the visual motion areas MT/MST (Boussaoud et al., 1990; Stanton et al., 1995, 2005) and the known implication of MT/MST in motion processing support the view that the frontal activity found during motion binding could be related to the FEF region. Also, the diversity of neural activities in the FEF region, including motor neurons, visuo-motor neurons and notably purely visuals neurons (Kirchner et al., 2009; Peng et al., 2008)and its implication in spatial attention, visual short term memory (Takahama et al., 2010; Tark and Curtis, 2009) or perceptual decision (Ferrera et al., 2009) question the exclusive implication of the FEF in oculomotor behavior and point to a wider functional role of FEF in visual processing than previously thought. Of interest for the present discussion is the recent finding of an implication of FEF in motion processing and anticipation (Ferrera et al., 2009) as well as a neuronal selectivity for 2D form (Kirchner et al., 2009; Peng et al., 2008). If the enhanced intermodulation term for bound trials was tied to SEF or FEF, this would rise the intriguing possibility that perceptual binding for overt or covert action (as discussed in the previous section) is characterized by a specific neural signature in the frequency domain. At least, the present data indicate that frequency-tagging with moving displays elicits specific enhanced power at the intermodulation frequency thus providing an electrophysiological marker of form/motion binding.

4. Experimental procedures

4.1. *Participants*

Twelve naive right-handed volunteers with normal vision took part in the study (6 women and 6 men, mean age 29.3±9.1 years). All participants provided informed written

consent and received a financial compensation for their participation. All procedures were approved by the local research ethics committee (Comité de Protection des Personnes Île-de-France VI, Paris, France).

4.2. *Stimuli and procedure*

The stimuli were presented via a mirror at the center of a rear projection screen using a calibrated video projector (1024×768 pixels; refresh rate, 60 Hz) located outside the shielded recording room. The distance between subjects' eyes and the screen was 0.85 m. The stimuli were composed of two pairs of horizontal and vertical bars (mean luminance 45.7 cd/m^2; length 5.0° of visual angle, dva thereafter; mean distance from the center 3 dva) displayed on a gray background (mean luminance 23.6 cd/m^2) and distributed so as to form a square shape (6.8×6.8 dva) with invisible corners around the central fixation point (Fig. 1b). The bars could remain static or move as follows: the horizontal bars oscillated in phase along a vertical axis at f1=2.3 Hz, while the vertical bars oscillated in phase along a horizontal axis at f2=3 Hz. This stimulus was expected to trigger the responses of direction selective cells at different harmonics of the bar motion frequencies, thus allowing the identification of neural populations responding to the vertical and horizontal motions. After our hypotheses, responses at intermodulation frequencies should reveal neural populations responding to a combination of these component motions. With oscillatory motion frequencies of 2.3 and 3 Hz, the first harmonics are 4.6 and 6 Hz and the 2f1+2f2 intermodulation term is 10.6 Hz. Motion amplitude was identical for the horizontal and vertical motion and equal to 1.2 dva.

As the perceptual binding of the component motions into a rigid moving shape is known to depend on the luminance ratio between the center and line ends of the bars (Lorenceau and Shiffrar, 1992), we designed four conditions, each characterized by a triangular distribution of luminance along the bars, as shown in Fig. 1a. High-luminance line ends yield a percept of unbound moving bars, while low-luminance line ends favor the perception of a bound shape. Preliminary behavioral experiments were conducted to choose luminance distributions yielding graded percepts: from strongly bound (condition 1) to completely unbound (condition 4). Note that the mean luminance of the bars is identical in all conditions. These stimuli, when static, are hardly discriminated on the sole basis of their luminance distribution (Fig. 1). In contrast, when moving, the different stimuli elicited highly discriminable perceptual states: a square with invisible corners moving along a Lissajou's trajectory – a rigid bound percept – or bars moving independently along the vertical and horizontal axes — a deforming unbound percept. Note that when asked whether they noticed the differences in luminance distribution, only one observer (not included in the analyses) among the twelve that performed noticed these differences.

Experimental trials comprised four periods as follows: A fixation point is first presented on the screen for 1.5 s (t=−1.5 to t=0). At t=0, four static bars are displayed for a duration varying randomly between 450 and 550 ms. This static phase is directly followed by 1.2 s of motion where both pairs of bars move sinusoidally along their orthogonal axis. Finally, a response screen with three color-coded circles displayed side by side is presented to indicate which response is associated with each button of the mouse: black for a rigidly moving square — bound percept; white for independent bar motions — unbound percept; gray for an indecipherable percept or to signal an intrusive perceptual switch — "unclassified trials" thereafter. In order to minimize artifacts associated with motor preparation, the horizontal positions of the three circles were randomly shuffled on each trial so that observers had to wait for the response screen to encode their motor response. Each subject underwent 8 runs of 60 trials each (15 trials per condition) for a total of 120 trials per condition.

4.3. *MEG recordings*

Continuous magnetoencephalographic signals were collected at a sampling rate of 1250 Hz, using a whole-head MEG system with 151 axial gradiometers (CTF Systems, Port Coquitlam, British Columbia, Canada), and low-pass filtered on-line at 300 Hz. Before each run, head localization was measured with respect to the MEG sensors using marker coils that were placed at the cardinal points of the head (nasion, left and right ears). Eye movements were recorded with an ISCAN eye-tracking system (240 Hz sampling rate). We also recorded the signal of a photodiode that precisely detected when the bars appeared on the screen. This allowed us to correct for the time delays introduced by the video projector (~24 ms) and to compute event-related magnetic fields (ERFs) precisely time-locked to the real stimulus onset.

4.4. *Data analysis*

Data were first pre-processed using both CTF and in-house software (http://cogimage.dsi.cnrs.fr/logiciels/). Trials contaminated by eye movements, blinks, or muscular artifacts were rejected off-line on visual inspection of ocular and MEG traces. Time zero was set at the onset of motion as obtained from the photodiode signal. Global analyses were performed on all trials independent of observers' percepts. Contrasts of MEG activity were computed between bound and unbound trials, as classified by the observers; unclassified trials were discarded from these analyses.

Most analyses were performed on averaged signals (SSVEF) but some were also performed on a trial-by-trial basis in order to highlight activity that may not be time-locked to the stimulation.

4.4.1. *Time–frequency analysis*

A time–frequency wavelet transform was applied on both the averaged SSVEF and a trial-by-trial basis in order to respectively analyze the evoked frequency components phase-locked to stimulus and the induced components non-phase locked to the stimulus (Tallon-Baudry and Bertrand, 1999). The wavelet transforms were computed for each MEG sensor using a family of complex Morlet wavelets (m=10), resulting in an estimate of the signal power for each time sample and each frequency between 1 and 100 Hz with a resolution varying with the frequency (Wf=0.235f in frequency and Wt=3.74/f in time). We focused the analysis on the range of the tagging frequencies (1–15 Hz; frequency step, 0.2 Hz) and the gamma band (40–100 Hz; frequency step, 2 Hz).

4.4.2. *Statistical tests performed on the time–frequency analyses*
Significance of the differences in all performed contrasts was established using a nonparametric cluster randomization test across spatial domain (Maris and Oostenveld, 2007; Nichols and Holmes, 2002). This test effectively controls the false discovery rate in situations involving multiple comparisons by clustering neighboring quantities that exhibit the same effect. For the amplitude analysis, the neighborhood was univariate across space (adjacent sensor over the scalp). The permutation method exhibits values whose t statistics exceeded a given critical value when comparing two conditions value by value. In order to correct for multiple comparisons, neighbor values exceeding the critical value were considered as a member of the same cluster. We take the usual critical value of 2 (Maris and Oostenveld, 2007). The cluster-statistic (CS) was taken as the size of each given cluster. Evaluating the cluster-statistic distribution through 1000 permutations controlled the false discovery rate (Pantazis et al., 2005). Each permutation represents a randomization of the data between the two conditions and across multiple subjects. For each permutation the cluster-statistics were computed by taking the cluster with the maximum size. The threshold that controls the family wise error rate (FWER) was determined according to the proportion of the randomization null distribution exceeding the observed maximum cluster-statistic (Monte Carlo test).

4.4.3. *Source modeling*
For each significant difference found at the sensor level, we reconstructed the sources of the activity to localize the corresponding brain regions. Sources of the MEG signals were estimated with the BrainStorm software (http://neuroimage.usc.edu/brainstorm) using a spherical head volume conductor and the cortical template "Colin27" of the Montreal Neurological Institute (MNI, http://www.bic.mni.mcgill.ca/). Co-registration of the anatomical template with the MEG coordinate system was achieved for each subject by aligning the positions of 3 reference coils with their corresponding anatomical landmarks (nasion and pre-auricular points). The MEG source imaging consisted of elementary ECD 10,000 sources distributed at each cortical node and normal to the cortical tessellation (Baillet et al., 2001). We used a minimum-L2-norm approach (Hämäläinen et al., 1993) to obtain one time course for each subject, condition and node of the cortical tessellation. As the duration of the motion onset asynchrony varied from trial to trial, SSVEFs were triggered to motion onset before averaging. For each of the 8 runs and for each subject, the responses were averaged across all trials and separately for bound and unbound trials. For each subject, the corresponding global responses were obtained with a weighted averaged across the runs with respect to the numbers of trials of each category. This methodology takes head position recorded at the beginning of each run into account to enhance the precision of the reconstruction.

4.4.4. *Spectral analysis on source time courses*
For the cortical source time courses (SSVEF), we estimated the power spectrum over two periods, one during the static display (baseline) and the other one during motion stimulation. This spectral analysis was performed using a Welch's periodogram (Marple, 1987) associated with Hamming windows. The analysis of the stimulation period was conducted on the last 1030 ms of the moving stimulus so as to exclude the expected M100 component following motion onset. The baseline signal was estimated on a time window of same size, from −1700 ms to −670 ms before motion onset. Given these parameters, the frequency resolution was 0.61 Hz for all spectral analyses. A base-2 log-transformed ratio of the signal power relative to the baseline was taken as the measure of interest; log-transformed data approach a normal distribution prior to performing statistical analysis, allowing the use of standard parametric tests to assess the statistical significance of the observed effects (Kiebel et al., 2005). Power spectrum estimations were also performed on the eye-movement data, in order to assess potential differences in oculomotor behavior depending on observer's perceptual state (bound or unbound).

Supplementary materials related to this article can be found online at doi:10.1016/j.brainres.2011.05.051.

Acknowledgments

C.A. was supported by a MRT grant. JL was supported by a grant ACI "Temps and Cerveau". We wish to warmly acknowledge the contribution of Antony Norcia who originally provided the rationale for this study.

REFERENCES

Ales, J.M., Norcia, A.M., 2009. Assessing direction-specific adaptation using the steady-state visual evoked potential: results from EEG source imaging. J. Vis. 9, 8.

Appelbaum, L.G., Wade, A.R., Pettet, M.W., Vildavski, V.Y., Norcia, A.M., 2008. Figure–ground interaction in the human visual cortex. J. Vis. 8, 8.1–8.19.

Aspell, J.E., Wattam-Bell, J., Atkinson, J., Braddick, O.J., 2010. Differential human brain activation by vertical and horizontal global visual textures. Exp. Brain Res. 202, 669–679.

Avery, G., Day, R., 1969. Basis of the horizontal–vertical illusion. Journal of Experimental Psychology 81, 376–380.

Baillet, S., Mosher, J., Leahy, R., 2001. Electromagnetic brain mapping. IEEE Signal Process. Mag. 18, 14–30.

Bardouille, T., Picton, T.W., Ross, B., 2006. Correlates of eye blinking as determined by synthetic aperture magnetometry. Clin. Neurophysiol. 117, 952–958.

Barlow, H.B., 1972. Single units and sensation: a neuron doctrine for perceptual psychology? Perception 1, 371–394.

Bosman, C.A., Womelsdorf, T., Desimone, R., Fries, P., 2009. A microsaccadic rhythm modulates gamma-band synchronization and behavior. J. Neurosci. 29, 9471–9480.

Boussaoud, D., Ungerleider, L.G., Desimone, R., 1990. Pathways for motion analysis: cortical connections of the medial superior temporal and fundus of the superior temporal visual areas in the macaque. J. Comp. Neurol. 296, 462–495.

Brignani, D., Maioli, C., Maria Rossini, P., Miniussi, C., 2007. Event-related power modulations of brain activity preceding visually guided saccades. Brain Res. 1136, 122–131.

Busch, N.A., Herrmann, C.S., Müller, M.M., Lenz, D., Gruber, T., 2006. A cross-laboratory study of event-related gamma activity in a standard object recognition paradigm. Neuroimage 33, 1169–1177.

Carrasco, M., Ling, S., Read, S., 2004. Attention alters appearance. Nat. Neurosci. 7, 308–313.

Castelo-Branco, M., Goebel, R., Neuenschwander, S., Singer, W., 2000. Neural synchrony correlates with surface segregation rules. Nature 405, 685–689.

Castelo-Branco, M., Formisano, E., Backes, W., Zanella, F., Neuenschwander, S., Singer, W., Goebel, R., 2002. Activity patterns in human motion-sensitive areas depend on the interpretation of global motion. Proc. Natl. Acad. Sci. U. S. A. 99, 13914–13919.

Cottereau, B., Lorenceau, J., Gramfort, A., Clerc, M., Thirion, B., Baillet, S., 2011. Phase delays within visual cortex shape the response to steady-state visual stimulation. Neuroimage 54, 1919–1929.

Culham, J.C., Brandt, S.A., Cavanagh, P., Kanwisher, N.G., Dale, A.M., Tootell, R.B., 1998. Cortical fMRI activation produced by attentive tracking of moving targets. J. Neurophysiol. 80, 2657–2670.

Dimigen, O., Valsecchi, M., Sommer, W., Kliegl, R., 2009. Human microsaccade-related visual brain responses. J. Neurosci. 29, 12321–12331.

Engbert, R., 2006. Microsaccades: a microcosm for research on oculomotor control, attention, and visual perception. Prog. Brain Res. 154, 177–192.

Ferrera, V.P., Yanike, M., Cassanello, C., 2009. Frontal eye field neurons signal changes in decision criteria. Nat. Neurosci. 12, 1458–1462.

Freunberger, R., Fellinger, R., Sauseng, P., Gruber, W., Klimesch, W., 2009. Dissociation between phase-locked and nonphase-locked alpha oscillations in a working memory task. Hum. Brain Mapp. 30, 3417–3425.

Friedman-Hill, S., Maldonado, P.E., Gray, C.M., 2000. Dynamics of striate cortical activity in the alert macaque: I. Incidence and stimulus-dependence of gamma-band neuronal oscillations. Cereb. Cortex 10, 1105–1116.

Fries, P., 2009. Neuronal gamma-band synchronization as a fundamental process in cortical computation. Annu. Rev. Neurosci. 32, 209–224.

Fries, P., Reynolds, J.H., Rorie, A.E., Desimone, R., 2001. Modulation of oscillatory neuronal synchronization by selective visual attention. Science 291, 1560–1563.

Fries, P., Schröder, J., Roelfsema, P.R., Singer, W., Engel, A.K., 2002. Oscillatory neuronal synchronization in primary visual cortex as a correlate of stimulus selection. J. Neurosci. 22, 3739–3754.

Gattass, R., Gross, C.G., 1981. Visual topography of striate projection zone (MT) in posterior superior temporal sulcus of the macaque. J. Neurophysiol. 46, 621–638.

Gray, C.M., Singer, W., 1989. Stimulus-specific neuronal oscillations in orientation columns of cat visual cortex. Proc. Natl. Acad. Sci. U. S. A. 86, 1698–1702.

Gray, C.M., Konig, P., Engel, A.K., Singer, W., 1989. Oscillatory responses in cat visual cortex exhibit inter-columnar synchronization which reflects global stimulus properties. Nature 338, 334–337.

Gruber, T., Trujillo-Barreto, N.J., Giabbiconi, C., Valdés-Sosa, P.A., Müller, M.M., 2006. Brain electrical tomography (BET) analysis of induced gamma band responses during a simple object recognition task. Neuroimage 29, 888–900.

Guo, K., Robertson, R., Nevado, A., Pulgarin, M., Mahmoodi, S., Young, M.P., 2006. Primary visual cortex neurons that contribute to resolve the aperture problem. Neuroscience 138, 1397–1406.

Hadjipapas, A., Adjamian, P., Swettenham, J.B., Holliday, I.E., Barnes, G.R., 2007. Stimuli of varying spatial scale induce gamma activity with distinct temporal characteristics in human visual cortex. Neuroimage 35, 518–530.

Hagler, D.J., Sereno, M.I., 2006. Spatial maps in frontal and prefrontal cortex. Neuroimage 29, 567–577.

Hämäläinen, M., Hari, R., Ilmoniemi, R.J., Knuutila, J., Lounasmaa, O.V., 1993. Magnetoencephalography—theory, instrumentation, and applications to noninvasive studies of the working human brain. Rev. Mod. Phys. 65, 413.

Henrie, J.A., Shapley, R., 2005. LFP power spectra in V1 cortex: the graded effect of stimulus contrast. J. Neurophysiol. 94, 479–490.

Herrmann, C.S., Senkowski, D., Röttger, S., 2004a. Phase-locking and amplitude modulations of EEG alpha: two measures reflect different cognitive processes in a working memory task. Exp. Psychol. 51, 311–318.

Herrmann, C.S., Munk, M.H., Engel, A.K., 2004b. Cognitive functions of gamma-band activity: memory match and utilization. Trends Cogn. Sci. 8, 347–355.

Hsieh, P., Tse, P.U., 2009. Microsaccade rate varies with subjective visibility during motion-induced blindness. PLoS One 4, e5163.

Innocenti, G.M., 2009. Dynamic interactions between the cerebral hemispheres. Exp. Brain Res. 192, 417–423.

Jensen, O., Kaiser, J., Lachaux, J., 2007. Human gamma-frequency oscillations associated with attention and memory. Trends Neurosci. 30, 317–324.

Jovicich, J., Peters, R.J., Koch, C., Braun, J., Chang, L., Ernst, T., 2001. Brain areas specific for attentional load in a motion-tracking task. J. Cogn. Neurosci. 13, 1048–1058.

Kagan, I., Gur, M., Snodderly, D.M., 2008. Saccades and drifts differentially modulate neuronal activity in V1: effects of retinal image motion, position, and extraretinal influences. J. Vis. 8, 19.1–19.25.

Kawakami, O., Kaneoke, Y., Maruyama, K., Kakigi, R., Okada, T., Sadato, N., Yonekura, Y., 2002. Visual detection of motion speed in humans: spatiotemporal analysis by fMRI and MEG. Hum. Brain Mapp. 16, 104–118.

Keil, A., Müller, M.M., Ray, W.J., Gruber, T., Elbert, T., 1999. Human gamma band activity and perception of a gestalt. J. Neurosci. 19, 7152–7161.

Kiebel, S.J., Tallon-Baudry, C., Friston, K.J., 2005. Parametric analysis of oscillatory activity as measured with EEG/MEG. Hum. Brain Mapp. 26, 170–177.

Kinsey, K., Anderson, S.J., Hadjipapas, A., Holliday, I.E., 2011. The role of oscillatory brain activity in object processing and figure–ground segmentation in human vision. Int. J. Psychophysiol. 79 (3), 392–400.

Kirchner, H., Barbeau, E.J., Thorpe, S.J., Régis, J., Liégeois-Chauvel, C., 2009. Ultra-rapid sensory responses in the human frontal eye field region. J. Neurosci. 29, 7599–7606.

Klimesch, W., 1999. EEG alpha and theta oscillations reflect cognitive and memory performance: a review and analysis. Brain Res. Brain Res. Rev. 29, 169–195.

Klimesch, W., Schack, B., Schabus, M., Doppelmayr, M., Gruber, W., Sauseng, P., 2004. Phase-locked alpha and theta oscillations generate the P1–N1 complex and are related to memory performance. Cogn. Brain Res. 19, 302–316.

Komatsu, H., Wurtz, R.H., 1988. Relation of cortical areas MT and MST to pursuit eye movements. I. Localization and visual properties of neurons. J. Neurophysiol. 60, 580–603.

Lam, K., Kaneoke, Y., Gunji, A., Yamasaki, H., Matsumoto, E., Naito, T., Kakigi, R., 2000. Magnetic response of human extrastriate cortex in the detection of coherent and incoherent motion. Neuroscience 97, 1–10.

Laubrock, J., Engbert, R., Kliegl, R., 2008. Fixational eye movements predict the perceived direction of ambiguous apparent motion. J. Vis. 8, 13.1–13.17.

Lima, B., Singer, W., Chen, N., Neuenschwander, S., 2010. Synchronization dynamics in response to plaid stimuli in monkey V1. Cereb. Cortex 20, 1556–1573.

Lobel, E., Kahane, P., Leonards, U., Grosbras, M., Lehéricy, S., Le Bihan, D., Berthoz, A., 2001. Localization of human frontal eye fields: anatomical and functional findings of functional magnetic resonance imaging and intracerebral electrical stimulation. J. Neurosurg. 95, 804–815.

Lorenceau, J., Shiffrar, M., 1992. The influence of terminators on motion integration across space. Vision Res. 32, 263–273.

Lorenceau, J., Zago, L., 1999. Cooperative and competitive spatial interactions in motion integration. Vis. Neurosci. 16, 755–770.

Lorenceau, J., Shiffrar, M., Wells, N., Castet, E., 1993. Different motion sensitive units are involved in recovering the direction of moving lines. Vision Res. 33, 1207–1217.
Majaj, N.J., Carandini, M., Movshon, J.A., 2007. Motion integration by neurons in macaque MT is local, not global. J. Neurosci. 27, 366–370.
Maris, E., Oostenveld, R., 2007. Nonparametric statistical testing of EEG- and MEG-data. J. Neurosci. Methods 164, 177–190.
Marple, S.L., 1987. Digital Spectral Analysis with Applications. [WWW Document]. URL http://adsabs.harvard.edu/abs/1987ph....book.....M.
Martinez-Conde, S., Macknik, S.L., Hubel, D.H., 2000. Microsaccadic eye movements and firing of single cells in the striate cortex of macaque monkeys. Nat. Neurosci. 3, 251–258.
Mikami, A., Newsome, W.T., Wurtz, R.H., 1986. Motion selectivity in macaque visual cortex. II. Spatiotemporal range of directional interactions in MT and V1. J. Neurophysiol. 55, 1328–1339.
Milner, P.M., 1974. A model for visual shape recognition. Psychol. Rev. 81, 521–535.
Min, B., Busch, N.A., Debener, S., Kranczioch, C., Hanslmayr, S., Engel, A.K., Herrmann, C.S., 2007. The best of both worlds: phase-reset of human EEG alpha activity and additive power contribute to ERP generation. Int. J. Psychophysiol. 65, 58–68.
Movshon, A., Adelson, E.H., Gizzi, M.S., Newsome, W.T., 1985. The analysis of moving visual patterns. In: Chagas, C., Gattass, R., Gross, C. (Eds.), Pattern Recognition Mechanisms: Pontificiae Academiae Scientiarum Scripta Varia, 54, pp. 117–151.
Nichols, T.E., Holmes, A.P., 2002. Nonparametric permutation tests for functional neuroimaging: a primer with examples. Hum. Brain Mapp. 15, 1–25.
Nowak, L.G., Munk, M.H., Nelson, J.I., James, A.C., Bullier, J., 1995. Structural basis of cortical synchronization. I. Three types of interhemispheric coupling. J. Neurophysiol. 74, 2379–2400.
Pack, C.C., Livingstone, M.S., Duffy, K.R., Born, R.T., 2003. End-stopping and the aperture problem: two-dimensional motion signals in macaque V1. Neuron 39, 671–680.
Palanca, B.J.A., DeAngelis, G.C., 2005. Does neuronal synchrony underlie visual feature grouping? Neuron 46, 333–346.
Pantazis, D., Nichols, T.E., Baillet, S., Leahy, R.M., 2005. A comparison of random field theory and permutation methods for the statistical analysis of MEG data. Neuroimage 25, 383–394.
Paus, T., 1996. Location and function of the human frontal eye-field: a selective review. Neuropsychologia 34, 475–483.
Pei, F., Pettet, M.W., Norcia, A.M., 2002. Neural correlates of object-based attention. J. Vis. 2, 588–596.
Peng, X., Sereno, M.E., Silva, A.K., Lehky, S.R., Sereno, A.B., 2008. Shape selectivity in primate frontal eye field. J. Neurophysiol. 100, 796–814.
Posthuma, D., Neale, M., Boomsma, D., de Geus, E., 2001. Are smarter brains running faster? Heritability of alpha peak frequency, IQ, and their interrelation. Behav. Genet. 31, 567–579.
Regan, M., Regan, D., 1988. A frequency domain technique for characterizing nonlinearities in biological systems. J. Theor. Biol. 133, 293–317.
Revonsuo, A., Wilenius-Emet, M., Kuusela, J., Lehto, M., 1997. The neural generation of a unified illusion in human vision. Neuroreport 8, 3867–3870.
Reynolds, J.H., Pasternak, T., Desimone, R., 2000. Attention increases sensitivity of V4 neurons. Neuron 26, 703–714.
Rodriguez, E., George, N., Lachaux, J.P., Martinerie, J., Renault, B., Varela, F.J., 1999. Perception's shadow: long-distance synchronization of human brain activity. Nature 397, 430–433.
Rust, N.C., Mante, V., Simoncelli, E.P., Movshon, J.A., 2006. How MT cells analyze the motion of visual patterns. Nat. Neurosci. 9, 1421–1431.
Sceniak, M.P., Ringach, D.L., Hawken, M.J., Shapley, R., 1999. Contrast's effect on spatial summation by macaque V1 neurons. Nat. Neurosci. 2, 733–739.
Siegel, M., Donner, T.H., Oostenveld, R., Fries, P., Engel, A.K., 2007. High-frequency activity in human visual cortex is modulated by visual motion strength. Cereb. Cortex 17, 732–741.
Simoncelli, E.P., Heeger, D.J., 1998. A model of neuronal responses in visual area MT. Vision Res. 38, 743–761.
Singer, W., Gray, C.M., 1995. Visual feature integration and the temporal correlation hypothesis. Annu. Rev. Neurosci. 18, 555–586.
Snodderly, D.M., Kagan, I., Gur, M., 2001. Selective activation of visual cortex neurons by fixational eye movements: implications for neural coding. Vis. Neurosci. 18, 259–277.
Stanton, G.B., Bruce, C.J., Goldberg, M.E., 1995. Topography of projections to posterior cortical areas from the macaque frontal eye fields. J. Comp. Neurol. 353, 291–305.
Stanton, G.B., Friedman, H.R., Dias, E.C., Bruce, C.J., 2005. Cortical afferents to the smooth-pursuit region of the macaque monkey's frontal eye field. Exp. Brain Res. 165, 179–192.
Sutoyo, D., Srinivasan, R., 2009. Nonlinear SSVEP responses are sensitive to the perceptual binding of visual hemifields during conventional 'eye' rivalry and interocular 'percept' rivalry. Brain Res. 1251, 245–255.
Swettenham, J.B., Muthukumaraswamy, S.D., Singh, K.D., 2009. Spectral properties of induced and evoked gamma oscillations in human early visual cortex to moving and stationary stimuli. J. Neurophysiol. 102, 1241–1253.
Takahama, S., Miyauchi, S., Saiki, J., 2010. Neural basis for dynamic updating of object representation in visual working memory. Neuroimage 49, 3394–3403.
Tallon-Baudry, C., 2009. The roles of gamma-band oscillatory synchrony in human visual cognition. Front. Biosci. 14, 321–332.
Tallon-Baudry, Bertrand, 1999. Oscillatory gamma activity in humans and its role in object representation. Trends Cogn. Sci. (Regul. Ed.) 3, 151–162.
Tallon-Baudry, C., Bertrand, O., Wienbruch, C., Ross, B., Pantev, C., 1997. Combined EEG and MEG recordings of visual 40 Hz responses to illusory triangles in human. Neuroreport 8, 1103–1107.
Tark, K., Curtis, C.E., 2009. Persistent neural activity in the human frontal cortex when maintaining space that is off the map. Nat. Neurosci. 12, 1463–1468.
Thiele, A., Stoner, G., 2003. Neuronal synchrony does not correlate with motion coherence in cortical area MT. Nature 421, 366–370.
Treisman, A.M., Gelade, G., 1980. A feature-integration theory of attention. Cogn. Psychol. 12, 97–136.
Tsui, J.M.G., Hunter, J.N., Born, R.T., Pack, C.C., 2010. The role of V1 surround suppression in MT motion integration. J. Neurophysiol. 103, 3123–3138.
Van Essen, D.C., Anderson, C.H., Felleman, D.J., 1992. Information processing in the primate visual system: an integrated systems perspective. Science 255, 419–423.
Varela, F., Lachaux, J.P., Rodriguez, E., Martinerie, J., 2001. The brainweb: phase synchronization and large-scale integration. Nat. Rev. Neurosci. 2, 229–239.
Victor, J.D., Conte, M.M., 2000. Two-frequency analysis of interactions elicited by Vernier stimuli. Vis. Neurosci. 17, 959–973.
Wandell, B.A., Dumoulin, S.O., Brewer, A.A., 2007. Visual field maps in human cortex. Neuron 56, 366–383.
Yazdanbakhsh, A., Livingstone, M.S., 2006. End stopping in V1 is sensitive to contrast. Nat. Neurosci. 9, 697–702.
Yuval-Greenberg, S., Tomer, O., Keren, A.S., Nelken, I., Deouell, L.Y., 2008. Transient induced gamma-band response in EEG as a manifestation of miniature saccades. Neuron 58, 429–441.
Zemon, V., Ratliff, F., 1984. Intermodulation components of the visual evoked potential: responses to lateral and superimposed stimuli. Biol. Cybern. 50, 401–408.